

Brief Report

The Effect of Azithromycin Plus Zinc Sulfate on ACE2 Expression through $\text{I}\kappa\text{B}\alpha$ of Human Respiratory Cells in SARS-CoV-2: In Vitro Study

Chia-Wei Chang¹, Ming-Cheng Lee², Bor-Ru Lin^{2,3}, Yen-Pei Lu¹, Yih-Jen Hsu², Chun-Yu Chuang⁴, Tsung-Tao Huang^{1,*} and Yin-Kai Chen^{5,6,*} 

¹ National Applied Research Laboratories, Biomedical Platform and Incubation Service Division, Taiwan Instrument Research Institute, Hsinchu 30261, Taiwan; 1909967@narlabs.org.tw (C.-W.C.); ypl@itrc.narl.org.tw (Y.-P.L.)

² Department of Internal Medicine, National Taiwan University Hospital, Taipei 10002, Taiwan; a0952008832@gmail.com (M.-C.L.); brucelin@ntuh.gov.tw (B.-R.L.); yihjen0805@gmail.com (Y.-J.H.)

³ Department of Integrated Diagnostics and Therapeutics, National Taiwan University Hospital, Taipei 10002, Taiwan

⁴ Department of Biomedical Engineering and Environmental Sciences, National Tsing Hua University, Hsinchu 30013, Taiwan; cychuang@mx.nthu.edu.tw

⁵ Graduate Institute of Clinical Medicine, College of Medicine, National Taiwan University, Taipei 10002, Taiwan

⁶ National Taiwan University Cancer Center, Department of Hematology, Taipei 10672, Taiwan

* Correspondence: tthuang@narlabs.org.tw (T.-T.H.); b8201032@tmu.edu.tw (Y.-K.C.); Tel.: +886-3-667-6822 (ext. 3063) (T.-T.H.); +886-2-2322-0322 (ext. 53996) (Y.-K.C.)



Citation: Chang, C.-W.; Lee, M.-C.; Lin, B.-R.; Lu, Y.-P.; Hsu, Y.-J.; Chuang, C.-Y.; Huang, T.-T.; Chen, Y.-K. The Effect of Azithromycin Plus Zinc Sulfate on ACE2 Expression through $\text{I}\kappa\text{B}\alpha$ of Human Respiratory Cells in SARS-CoV-2: In Vitro Study. *COVID* **2021**, *1*, 263–275. <https://doi.org/10.3390/covid1010021>

Academic Editors: Cheng-Wen Lin and Szu-Hao Kung

Received: 9 July 2021

Accepted: 19 August 2021

Published: 20 August 2021

Publisher's Note: MDPI stays neutral with regard to jurisdictional claims in published maps and institutional affiliations.



Copyright: © 2021 by the authors. Licensee MDPI, Basel, Switzerland. This article is an open access article distributed under the terms and conditions of the Creative Commons Attribution (CC BY) license (<https://creativecommons.org/licenses/by/4.0/>).

Abstract: Large-scale efforts have been persistently undertaken for medical prophylaxis and treatment of COVID-19 disasters worldwide. A variety of novel viral spike protein-targeted vaccines have been extensively distributed for global inoculation based on accelerated approval. With concerns of emerging spike protein mutations, we revisited the early but inconclusive clinical interest in the repurposed combination of azithromycin (AZT) and zinc supplements with safety advantages. The aim of this study is to provide in vitro proof of concept for $\text{I}\kappa\text{B}\alpha$ associated rapid and synergistic suppression of angiotensin-converting enzymes 2 (ACE2) following combination treatments with AZT plus zinc sulfate in two human airway cells with ACE2 expression, Calu-3 and H322M, representative cells of the human upper and lower airway origin respectively. Clinical timing of AZT combined with zinc is indicated based on suppression of the key cellular entry molecule, ACE2, of SARS-CoV-2.

Keywords: repurposing; COVID-19; viral entry

1. Introduction

Cell surface angiotensin-converting enzymes 2 (ACE2) of the respiratory tract is a well-established critical entry of SARS-CoV-2 into infected cells [1–3]. ACE2 mRNA expression was shown to be reduced from tracheobronchial to bronchioloalveolar regions [4]. ACE2 expression was upregulated following viral infection [5,6], interferon exposure [5,6], and smoking [5,6]. It has been postulated that hyperactivation of the transcription factor nuclear factor- κB (NF- κB) following ACE2-mediated viral entry, most likely in nonimmune cells, including lung epithelial cells, resulted in cytokine release syndrome [7]. Human type II pneumocytes (AT2) are one of the primary targets for SARS-CoV-2 infection [6]. It was shown in an induced pluripotent stem cell-derived AT2 model that NF- κB signaling was rapidly and persistently upregulated upon SARS-CoV-2 infection [8]. Delayed interferon (IFN) activation was also observed in the same model [8]. Increased blood type I IFN- α levels were reported 7 days after infection and indicated better clinical outcomes [9]. IFN- α , known to activate NF- κB pathway [10,11], also showed in vitro antiviral activity against

SARS-CoV-2 [12]. However, IFN- α increased ACE2 expression in primary nasal epithelial cells from healthy nasal mucosa and a human bronchial cell line [13]. Therefore, interaction between ACE2 and NF- κ B is worth explored and targeted for ACE2 suppression. With emerging threats of mutations located on the viral spike protein [14], blocking ACE2 for viral entry has become one of the major ways with prophylactic and early therapeutic attempts to prevent unpredictable inflammation induced by SARS-CoV-2 infection [15,16].

Among a variety of repurposed combinations for COVID-19, regimens containing azithromycin (AZT) [17–24] or zinc supplements [25] and in combinations [26,27] have drawn clinical attention since early outbreak. There was a trend toward better clinical outcomes in retrospective analysis for hydroxychloroquine (HCQ) plus AZT. A pilot observation study of 80 PCR-documented hospitalized patients with relatively mild disease treated with combination of 10-day HCQ and 5-day AZT reported high rate of clinical recovery as well as rapid and viral load clearance [18]. The largest retrospective analysis of 3737 PCR-documented patients treated with the same combination earlier also suggested better clinical outcomes and a faster viral load reduction [19]. Another similar retrospective study with 1061 PCR-documented patients also showed favorable clinical outcomes and a high rate of viral load clearance [23]. Only in one large retrospective cohort with 1438 lab-confirmed patients, in-hospital mortality was not reduced by HCQ with/without AZT [20]. However, clinical benefits of the HCQ/AZT combination were not shown in two representative prospective trials. In a multicenter, randomized, open-label controlled trial involving 667 suspected and confirmed hospitalized patients with mild-to-moderate COVID-19, 7-day HCQ with/without AZT did not improved clinical outcomes [17]. In another randomized, open-labeled trial for 447 hospitalized patients with severe suspected and confirmed COVID-19, AZT in addition to HCQ did not further improve clinical outcomes [24]. With regard to zinc supplement, a retrospective observation between HCQ/AZT with/without zinc sulfate for PCR-documented patients reported favorable clinical outcomes with addition of zinc sulfate [26]. In a retrospective case series, zinc combined with AZT and low-dose HCQ reduced hospitalization rate in PCR-documented risk-stratified community patients [27]. Besides, large-scale randomized trials did not reveal hydroxychloroquine's clinical benefits of in patients with COVID-19 [28,29]. Possibly due to inconclusive clinical roles and cardiac concerns [17,20,24], AZT monotherapy was ever explored in outpatient setting. A randomized, open-label controlled trial involving a larger proportion of suspected patients did not show clinical improvements after three-day outpatient AZT treatment [22]. A single high-dose outpatient AZT did not provide clinical benefits for lab-documented patients in a randomized, placebo-controlled trial [30]. Accordingly, the feasible clinical timing and combination choice with AZT remain unelucidated.

AZT, a second-generation macrolide with broad spectrum antibacterial activity, has drawn clinical attention in early pandemic among hot drug repurposing for the recurrence of COVID-19 patients [17–20]. In addition to its antimicrobial activity resulting from bacterial protein synthesis inhibition [31], AZT protects against viral entry into A549 lung cancer cell lines [32] and viral infections of airway epithelial cells through reduced viral replication and increased interferon responses [33–35]. AZT was demonstrated in vivo to suppress NF- κ B activation and concomitant pulmonary inflammation [36]. Tumor-necrosis factor- α (TNF- α)-induced NF- κ B DNA binding activity, NF- κ B inhibitor alpha ($\text{I}\kappa\text{B}\alpha$) degradation and interleukin-6 (IL-6)/IL-8 release in tracheal cells of human origin were shown to be dose-dependently inhibited in vitro following AZT [37].

Zinc is a trace element supplement with clinical benefits in respiratory tract infections [38]. Zinc deficiency prevalence of 26% was ever reported in a case-control study of adults aged 50 years or older visiting an Ohio outpatient clinic between 2014 and 2017 [39]. Patients with COVID-19 had significantly lower serum zinc levels than normal controls [40]. More complications are developed in COVID-19 patients with zinc deficiency [40]. The prophylactic and therapeutic roles of zinc supplementation are currently under investigation [41,42]. Prevention of viral entry has been postulated to be a potential mechanism

for zinc antiviral actions [38]. Increased NF- κ B DNA binding activity and I κ B α mRNA expression were reported in lungs from a septic mouse model with zinc deficiency [43].

Based on hypothesis of I κ B α -mediated ACE2 suppression for viral entry to human airway cells, the aim of this study was to explore in vitro if synergistic ACE2 suppression played a role in the underlying mechanism of the two potential I κ B α modulators, AZT, a zinc ionophore [26], and zinc sulfate. Importantly, it was expected to provide first laboratory support for clinical timing of the repurposed AZT plus zinc early in the outbreak for COVID-19 with less clinical safety concerns of I κ B α modulation.

2. Materials and Methods

2.1. Cell Lines

Because airway is the primary and lethal target involved in COVID-19, Calu-3, H322M, H522, H460, H1299, and A549 human airway cells were screened in this study for endogenous ACE2 expression. H322M, H522, H460, and A549 human airway cells were courtesy of SLY (National Taiwan University, Taipei, Taiwan), and H1299 lung cancer cell line was courtesy of CCH (National Taiwan University Hospital, Taipei, Taiwan). Calu-3 human upper airway cells were purchased from the American Type Culture Collection (ATCC) (Manassas, VA, USA). The Calu-3 cells were cultured with Minimum Essential Media (MEM) (Thermo Fisher Scientific, Waltham, MA, USA) containing 20% (*v/v*) fetal bovine serum (Thermo Fisher Scientific, Waltham, MA, USA), 100 mM sodium pyruvate, nonessential amino acids and penicillin-streptomycin in a humidified 5% CO₂ atmosphere. The H322M cells were cultured with Roswell Park Memorial Institute (RPMI) medium (Thermo Fisher Scientific, Waltham, MA, USA) containing 10% (*v/v*) fetal bovine serum (Thermo Fisher Scientific, Waltham, MA, USA) and penicillin-streptomycin at 37 °C in a humidified 5% CO₂ atmosphere.

2.2. Drug Treatments

In order to screen the potential and dose of Zn and AZT for rapid ACE2 mRNA suppression, H322M was seeded at a density of 5×10^5 cells per 6-well plate incubated for 20 h at 37 °C in 5% CO₂. The culture medium was removed and replaced with fresh medium in the presence of 24 h serial doses of 18.75, 37.5, 75, 150, and 300 μ M Zn and 24 h serial doses of 50, 25, 12.5, 6.25 and 3.125 μ M AZT respectively.

After seeding at a density of 1×10^6 cells per 6-well plate, Calu-3 and H322M cells were incubated for 20 h at 37 °C in 5% CO₂ for combination treatments as follows. The culture medium was removed and replaced with fresh medium in the presence of (i) 1/1000 DMSO, (ii) 25 μ M AZT (MCE, Monmouth Junction, NJ, USA), (iii) 50 μ M AZT, and (iv) 300 μ M Zinc Sulfate, ZnSO₄ (Zn) (Sigma-Aldrich, ST. Louis, MO, USA), (v) 300 μ M Zn and 25 μ M AZT, (vi) 300 μ M Zn and 50 μ M AZT, and incubated for 24 or 48 h.

2.3. RNA Isolation

Total RNA was isolated from each treatment and control group using the PureLink™ RNA mini kit (Thermo Fisher Scientific, Waltham, MA, USA) according to the manufacturer's instructions. The RNA concentration and quality were assessed using the Quibit 3.0 Fluorometer (Thermo Fisher Scientific, Waltham, MA, USA). Total RNA samples were stored at -80 °C.

2.4. Reverse Transcription (RT)

RT reactions were carried out using the superscript III first strand synthesis system (Thermo Fisher Scientific, Waltham, MA, USA). cDNA was synthesized starting from 2 μ g of purified total RNA. The reactions in a final volume of 20 μ L contained 1x Buffer, dithiothreitol (DTT), deoxy-ribonucleoside triphosphates (dNTPs), superscript III RT, and 500 ng oligo(dT). Samples were incubated at 65 °C for 5 min and 50 °C for 60 min, and

then the RT enzyme was inactivated by heating to 70 °C for 15 min. cDNA samples were stored at −20 °C.

2.5. Quantitative PCR (qPCR)

qPCR was carried out with KAPA SYBR®FAST qPCR Master Mix (Wilmington, MA, USA) in a final volume of 20 µL, with 0.3 µM forward and reverse primer and 1 µL of cDNA. Fluorescent detection was performed using the ABI 7500 fast System (Thermo Fisher Scientific, Waltham, MA, USA) with the following thermal cycling conditions: initial polymerase activation at 95 °C for 3 min, followed by 40 cycles of denaturation at 95 °C for 3 s and annealing/extension at 60 °C for 30 s. After amplification, dissociation (melting) curve analysis was performed to analyze the product melting temperature. Each sample was amplified in triplicate wells. Negative (no template) controls were included in each assay. The results were analyzed using ABI 7500 Fast System Software. The threshold cycle (Ct) at which the amount of amplified target reached a fixed threshold was determined. Relative expression was calculated using the $2^{-\Delta\Delta C_q}$ method. The results were analyzed and are shown as the fold change relative to each control group. Primers of our targets of interest, *ACE2*, *IKB α* , *MUC1* were listed in Table 1. Table 1 also included primers of internal control, *RPLP0*, for Calu-3 and *GAPDH* for H322M.

Table 1. Primers used for qPCR.

Gene	Primer Sequences (5'→3')	Product Size (bp)
<i>RPLP0</i>	F: TGGTCATCCAGCAGGTGTTCTGA R: ACAGACACTGGCAACATTGCGG	119
<i>GAPDH</i>	F: GAAGGTGAAGGTCCGAGT R: GAAGATGGTGTATGGGATTTC	172
<i>ACE2</i>	F: GGACCCAGGAAATGTTTCAGA R: GGCTGCAGAAAGTGACATGA	238
<i>IKBα</i>	F: GAAGTGATCCGCCAGGTGAA R: CTGCTCACAGGCAAGGTGTA	189
<i>MUC1</i>	F: CCTACCATCCTATGAGCGAGTAC R: GCTGGGTTTGTGTAAGAGAGGC	136

Abbreviation: ribosomal protein P0, RPLP0; glyceraldehyde-3-phosphate dehydrogenase, GAPDH; mucin-1, MUC1.

2.6. Western Blot

Cells were scraped with lysis buffer (1% Triton X-100, 20 mM Tris pH 7.4, 150 mM NaCl, and protease inhibitors) on an ice tray, and cell lysates were subjected to western blot analysis. Protein samples were first separated by SDS-PAGE and then transferred to a PVDF membrane. Primary antibodies were applied to detect specific protein expression, followed by incubation with appropriate HRP-conjugated secondary antibodies. Protein signals were developed using an enhanced chemiluminescence reagent (Biomate, Taipei, Taiwan) and detected by a BIO-RAD ChemiDoc™ MP imaging system (BIO-RAD, Hercules, CA, USA). Western blots were carried out with ACE-2 antibody (Bioss, Woburn, MA, USA), IKB- α antibody (Santa Cruz, Dallas, TX, USA), and PARP antibody (Cell Signaling, Danvers, MA, USA); α -tubulin antibody (Novus, Littleton, CO, USA) was used as a loading control.

2.7. Statistical Analysis

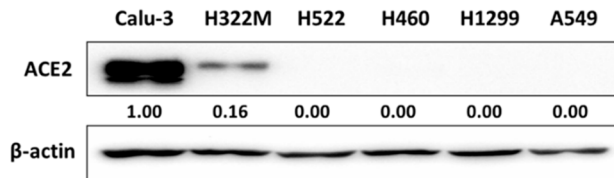
For statistical analysis, the mean and standard errors were calculated by using GraphPad Prism software version 9 (GraphPad Software Inc., San Diego, CA, USA). Student's t-tests were used to determine significant differences between two experimental conditions. $p < 0.05$ was considered to be significant for all experiments. Data were presented as mean + SEM.

3. Results

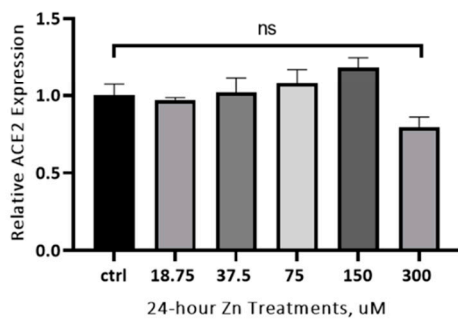
Endogenous ACE2 expressions were found in Calu-3 and H322M, with markedly abundant ACE2 expression in Calu-3 (Figure 1A). Therefore, Calu-3, widely used for

COVID-19 studies, and H322M were selected for subsequent exploration. Zn at 300 μM was determined for the subsequent drug repurposing combination study because *ACE2* mRNA suppression was observed following 24 h treatment of H322M (Figure 1B). An AZT concentration of 50 and 25 μM was chosen for Zn combination exploration because *ACE2* mRNA suppression was observed³ in H322M following 24 h treatment (Figure 1C).

A. Baseline ACE2 expression



B. Zn Dosing, H322M



C. AZT Dosing, H322M

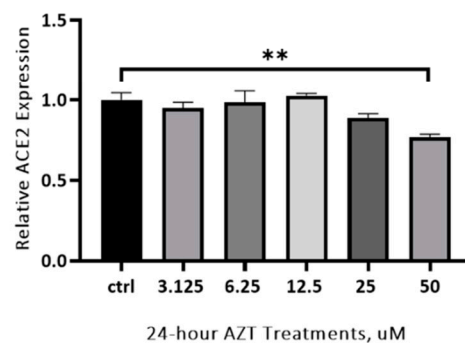


Figure 1. Azithromycin (AZT) but not ZnSO₄ (Zn) treatment alone decreased endogenous ACE2 expression in the human lower airway H322M cells. (A) Endogenous ACE2 expression was screened by Western blot using beta-actin as a loading control. ACE2-expressing Calu-3 and H322M cell lines were selected for subsequent exploration. (B) H322M cells were treated with serial concentrations of Zn (H₂O ctrl, 18.75, 37.5, 75, 150, and 300 μM) for 24 h, and total RNA was collected for ACE2 quantitation by real-time qRT-PCR assays. The data were normalized to *GAPDH* expression and presented as the mean \pm SEM ($n = 3$). ACE2 expression was potentially decreased under 24 h treatment with 300 μM Zn. This concentration was determined for combination treatment with AZT. (C) H322M cells were treated with a concentration series of AZT (DMSO ctrl, 3.125, 3.25, 12.5, 25, and 50 μM) for 24 h, and total RNA was collected for ACE2 quantitation by real-time qRT-PCR assays. The data were normalized to *GAPDH* expression and presented as the mean \pm SEM ($n = 3$). (** $p = 0.001$ to 0.01). ACE2 expression was significantly decreased under 24 h treatment with 50 μM AZT. This concentration was adopted for combination treatment with Zn.

This study’s most impressive finding was the rapidly suppressed endogenous *ACE2* mRNA and protein expressions of H322M under 24 h treatment of 300 μM Zn combined with 50 and 25 μM AZT (Figures 2A and 3A). Compared to control, 300 μM Zn in combination with 50 μM ($p = 0.0055$) and 25 μM AZT ($p = 0.0008$) significantly suppressed *ACE2* mRNA expression (Figure 3A). Compared to 50 and 25 μM AZT treatments alone in H322M, 300 μM Zn showed a significant synergistic suppressive effect on *ACE2* mRNA expression in combination with 50 μM ($p = 0.0207$), 25 μM AZT ($p < 0.0001$) (Figure 3A). *ACE2* protein expression in H322M was further decreased following 48 h treatment with Zn and AZT combinations, especially 50 μM AZT (Figure 2B). Compared to control in 24 h treated Calu-3, 300 μM Zn alone ($p = 0.0021$) and in combination with 50 μM ($p = 0.0007$) and 25 μM AZT ($p = 0.0018$) significantly suppressed *ACE2* mRNA expression (Figure 3C). *ACE2* mRNA expression of Calu-3 was significantly reduced following 24 h treatment of

300 μM Zn alone and in combination with 50 ($p = 0.0105$) and 25 ($p = 0.0029$) μM AZT (Figure 3C). The markedly suppressive effect on ACE2 protein expression in Calu-3 was found 24 h later following the suppression of ACE2 mRNA expression. Similar to H322M, 48 h combination treatment with 300 μM and 50 μM AZT showed the most suppressive effect on ACE2 expression in Calu-3 (Figure 2D). With regard to cytotoxic evaluation of AZT, Zn and in combinations, cleaved PARP, an indicator of apoptosis, was not detected across a variety of treatment groups.

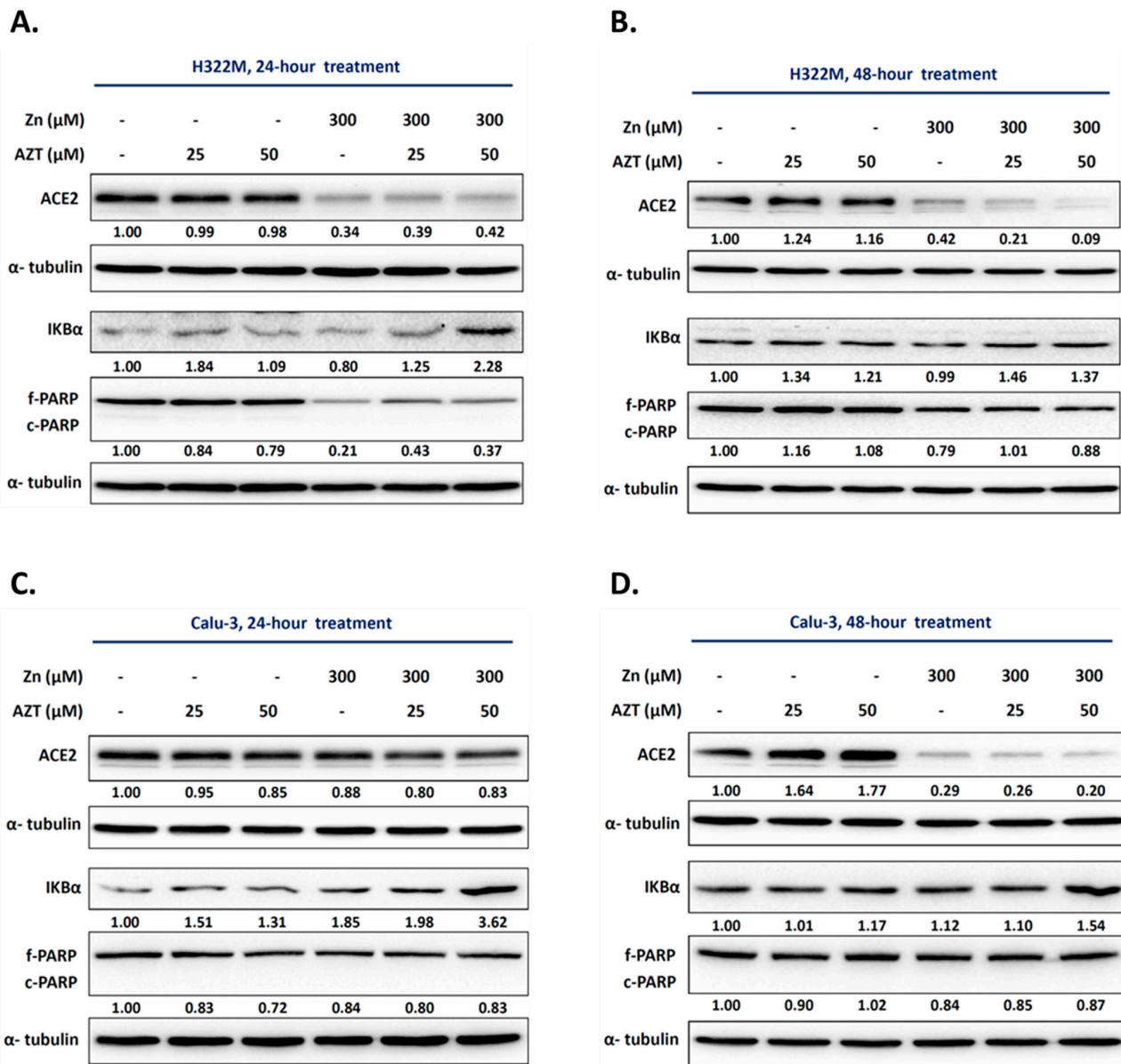


Figure 2. Endogenous ACE2 expression in H322M and Calu-3 cells was markedly suppressed by Zn and in combination with AZT in a time- and dose-dependent manner. (A,B) H322M cells were treated with DMSO ctrl, 25, 50 μM AZT and 300 μM Zn in combination for 24 (A) and 48 (B) hours. Treated cells were lysed for Western blot analysis of ACE2 and PARP with α -actin as a loading control. ACE2 expression was suppressed without detectable cleaved PARP by Zn alone and synergistically with AZT in a time- and dose-dependent manner. IKB- α expression was obviously increased following 24 h of treatment with 300 μM Zn combined with 50 μM AZT. (C,D) Calu-3 cells were treated with 25, 50 μM AZT and 300 μM Zn in combination for 24 (C) and 48 (D) hours. Compared to H322M treated in the same ways, ACE2 expression was suppressed without detectable cleaved PARP by Zn alone and synergistically with AZT in a more time-dependent manner. Similarly, IKB- α expression was obviously increased following 24 h of treatment with 300 μM Zn combined with 50 μM AZT.

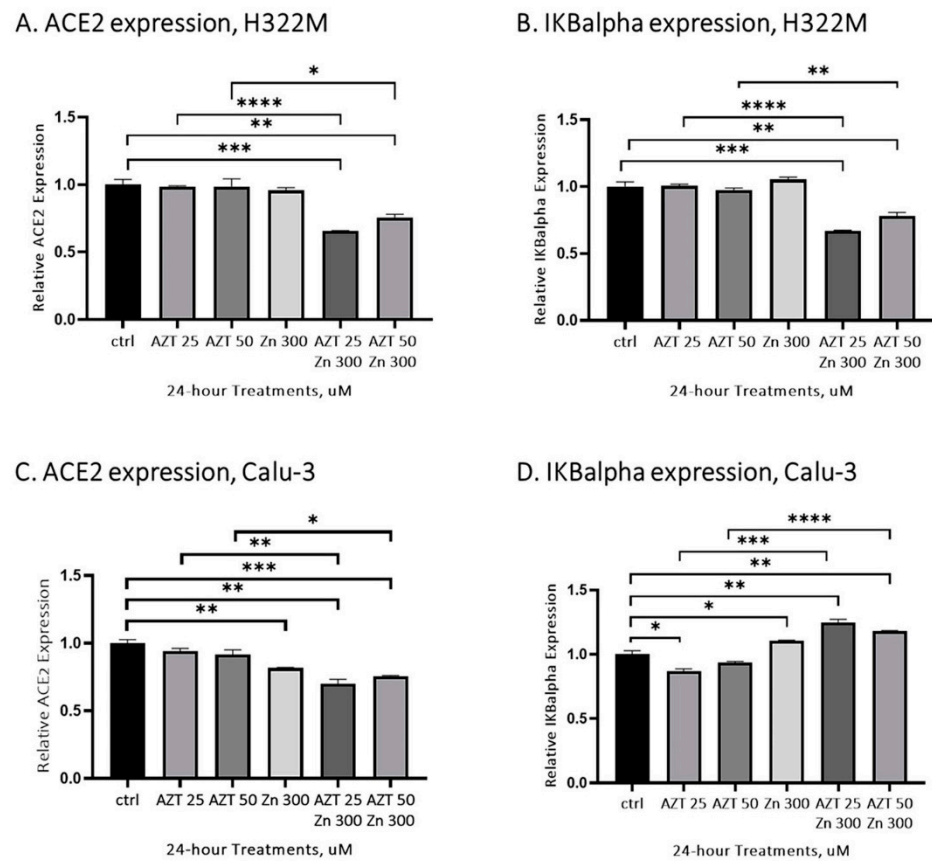


Figure 3. Endogenous ACE2 and IκBα expression was synergistically regulated by combined treatments of Zn and AZT. (A,B) H322M cells were treated with DMSO ctrl, 25, 50 μM AZT and 300 μM Zn in combination for 24 h. Total RNA was collected for ACE2 (A) and IκBα (B) quantitation by real-time qRT-PCR assays. The data were normalized to GAPDH expression and presented as the mean ± SEM (n = 3). (* p = 0.01 to 0.05, ** p = 0.001 to 0.01, *** p = 0.0001 to 0.001, and **** p = < 0.0001). Compared to AZT alone, 300 μM Zn synergistically decreased ACE2 and IκBα expression with 25 (ACE2 and IκBα, p < 0.001) and 50 μM (ACE2, p = 0.0207; IκBα = 0.0033) AZT treatments, respectively. (C,D) Calu-3 cells were treated with 25, 50 μM AZT and 300 μM Zn in combination for 24 h. Total RNA was collected for ACE2 (A) and IκBα (B) quantitation by real-time qRT-PCR assays. The data were normalized to GAPDH/RPLP0 expression for H322M/Calu-3 cells respectively and presented as the mean ± SEM (n = 3). (* p = 0.01 to 0.05, ** p = 0.001 to 0.01, *** p = 0.0001 to 0.001, and **** p = < 0.0001). Zn showed a similar synergistic suppressive effect on ACE2 expression in AZT treated Calu-3 cells. Conversely, IκBα expression was synergistically upregulated following 25 (p = 0.0003) and 50 (p < 0.0001) μM AZT treatments combined with 300 μM Zn compared to AZT alone.

Finally, our H322M-associated results indicated that Zn and AZT combination treatments altered IκBα degradation and contributed to rapid suppression of endogenous ACE2 (Figure 2A,B and Figure 3A,B). Such synergistic effects on IκBα degradation were most prominent following 24 h treatment with 300 μM Zn and 50 μM AZT (Figures 2A and 3B). Compared to control, IκBα mRNA expression was significantly reduced by 24 h 300 μM Zn in combination with 50 μM (p = 0.0081) and 25 μM AZT (p = 0.0008) (Figure 3B). Compared to 24 h 50 and 25 μM AZT treatments alone, 300 μM Zn showed a significant synergistic suppressive effect on IκBα mRNA expression in combination with 50 μM (p = 0.0033), 25 μM AZT (p < 0.0001) (Figure 3B). In contrast to the synergistic effect on IκBα degradation in H322M, IκBα mRNA and protein expressions in Calu-3 was rapidly upregulated following 24 h treatment of 300 μM Zn combined with 50 and 25 μM AZT (Figures 2C and 3D). Compared to control,

IκBα mRNA expression was significantly increased by 24 h 25 μM AZT ($p = 0.0172$), 300 μM Zn ($p = 0.023$) alone and in combination with 50 μM ($p = 0.003$) and 25 μM AZT ($p = 0.0027$) (Figure 3D). Compared to 24 h 50 and 25 μM AZT treatments alone, 300 μM Zn showed a significant synergistic upregulated effect on *IκBα* mRNA expression in combination with 50 μM ($p < 0.0001$), 25 μM AZT ($p = 0.0003$) (Figure 3D). A similar resultant synergistic ACE2 suppressive effect was most prominent following 48 h 300 μM Zn treatment combined with 50 μM AZT (Figure 2C,D). Membrane-tethered MUC1 belongs to one of the major components of mucus [44]. Elevated MUC1 mucin protein levels were found in the airway mucus of critically ill COVID-19 patients [45,46]. In addition to *IκBα*-mediated synergistic ACE2 suppression by AZT plus Zn, inflammation and respiratory distress associated mucus might be taken into consideration for optimal clinical timing of such repurposed combinations. Another interesting finding of this study was that *MUC1* mRNA expression in H322M and Calu-3 cells was most significantly increased following 24 h treatment with 300 μM Zn alone (H322M, $p < 0.0001$; Calu-3, $p = 0.0013$) and a lesser degree after combined treatment with 50 and 25 μM AZT (Figure 4A,B). Compared to control, *MUC1* mRNA expression of H322M was significantly increased by 24 h 300 μM Zn ($p < 0.0001$) alone and in combination with 50 μM ($p = 0.0077$) and 25 μM AZT ($p = 0.0279$) (Figure 4A). Compared to 24 h 50 μM AZT treatments alone, 300 μM Zn showed a significant synergistic upregulated effect on *MUC1* mRNA expression in combination with 50 μM ($p = 0.0082$) (Figure 4A). Compared to control, *MUC1* mRNA expression of Calu-3 was significantly increased by 24 h 300 μM Zn ($p = 0.0013$) and in combination with 50 μM ($p = 0.0014$) and 25 μM AZT ($p = 0.0024$) (Figure 4B). Compared to 24 h 50 and 25 μM AZT treatments alone, 300 μM Zn showed a significant synergistic upregulated effect on *MUC1* mRNA expression in combination with 50 μM ($p = 0.0014$) and 25 μM AZT ($p = 0.0086$) (Figure 4B).

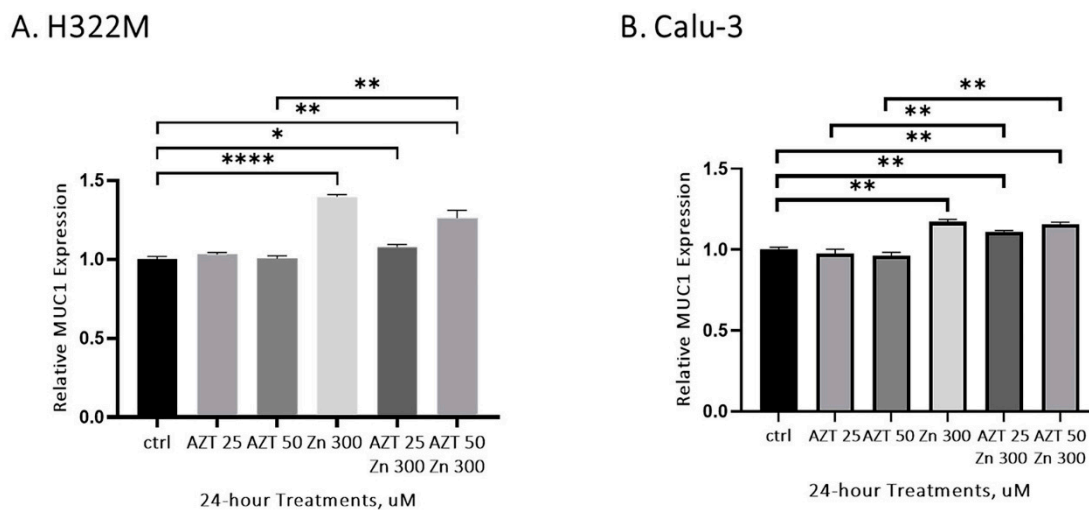


Figure 4. Endogenous MUC1 expression was significantly increased by Zn treatment alone and to a lesser degree in combination with AZT. H322M (A) and Calu-3 (B) cells were treated with 25, 50 μM AZT and 300 μM Zn in combination for 24 h. Total RNA was collected for MUC1 quantitation by real-time qRT-PCR assays. The data were normalized to GAPDH/RPLP0 expression for H322M/Calu-3 cells respectively and are presented as the mean ± SEM ($n = 3$). (* $p = 0.01$ to 0.05 , ** $p = 0.001$ to 0.01 , and **** $p < 0.0001$). Compared to the control, MUC1 expression was significantly increased following 300 μM Zn treatment alone (H322M, $p < 0.0001$; Calu-3, $p = 0.0013$) and to a lesser degree combined with AZT in H322M and Calu-3 cells. In H322M, MUC1 expression was synergistically increased following 50 μM AZT treatments combined with 300 μM Zn compared to AZT alone. In Calu-3 cells, MUC1 expression was synergistically increased following 25 and 50 μM AZT treatments combined with 300 μM Zn compared to AZT alone.

4. Discussion

Published clinical repurposing combinations containing AZT, zinc or in combinations are categorized into retrospective analysis and prospective clinical trials. One of major differences between the two categories is that patients in retrospective analysis are lab-documented COVID-19, but a small proportion of only clinically suspected COVID-19 patients were enrolled in prospective trials. Interestingly, clinical benefits of repurposed combinations shown in retrospective analysis were usually not reached in prospective trials. Due to concerns of cardiac events in HCQ component of combinations, this study is the first to present *in vitro* evidence that HCQ-free repurposed combination of AZT plus Zn rapidly and significantly suppresses endogenous ACE2 expression and increases MUC1 expression in Calu-3 and H322M cells. A published computed model of the AZT-Zinc ion complex demonstrated its potential against the replication and assembly of SARS-CoV-2 particles (doi:10.2174/1874091X02014010033). The Calu-3 cells generated from human proximal bronchial adenocarcinoma [47] are characterized by differentiated, functional human airway epithelial cells [48]. These cells were also proposed to be a suitable model for the human nasal mucosa [49]. Bronchoalveolar lavage analyses from COVID-19 patients disclosed aberrant macrophage and T cell responses [50] as well as bronchoalveolar immune hyperactivation [51]. Our drug repurposing for the critical bronchoalveolar involvement of COVID-19 was investigated with H322M, a bronchoalveolar cell line, in addition to Calu-3 for proximal airway involvement.

Symptoms, including fever, dyspnea and hypoxia, were rapidly improved following high-dose zinc rescue with different preparations in a consecutive COVID-19 case series [25]. A randomized placebo-controlled trial for high-dose intravenous zinc was initiated as adjunctive therapy in SARS-CoV-2-positive critically ill patients [52]. Although the targeted enrollment was not reached, the pilot report showed only minimal infusion site irritation in a small proportion of patients in treatment group [53]. Therefore, it is supposed clinically safe to supplement repurposed AZT with high-dose zinc. Interestingly, high-dose Zn alone in this study showed mild-to-moderate ACE2 suppression in Calu-3 and H322M.

Certain NF- κ B dimeric transcription factors and their activities are tightly repressed by three inhibitors, I κ B α , I κ B β , and I κ B ϵ , through the formation of stable I κ B-NF- κ B complexes. Zinc is supposed to be an I κ B α modulator with antiviral activities including viral entry prevention. It was demonstrated that rapid degradation of free I κ B α is critical for NF- κ B activation [54]. 50 μ M AZT induced significant *in vitro* anti-rhinoviral activities in normal primary bronchial epithelial cells [33] and those cells from children with cystic fibrosis [34]. Lower *in vitro* anti-rhinoviral levels of AZT were also reported for bronchial epithelial cells from patients with chronic obstructive lung disease [35]. In this study, I κ B α protein expressions were increased in Calu-3 and H322M following 24 h treatment of high-dose AZT of 50 μ M plus Zn. Progressively ACE2 suppression ensued from 24 h to 48 h treatments of the two cells with high-dose AZT plus Zn, indicative of sequential regulatory interaction between ACE2 and I κ B α . The different patterns of I κ B α mRNA changes in Calu-3 and H322M suggested endogenous cell-type specific regulatory effects of AZT and Zn in combinations. The concomitant increased I κ B α mRNA/protein in Calu-3 indicated increased protein expression following upregulated mRNA transcription by combination treatments. The inverse changes of I κ B α mRNA/protein in H322M supposed to be associated with decreased I κ B α degradation following combination treatments.

Hypoxia is a common threat in moderate-to-severe COVID-19. SARS-CoV-2 infection increased lung MUC1 expression and resulted in hypoxia in a mouse model [46]. In order to explore optimal clinical timing of the repurposed combination, this study revealed that 24 h high-dose Zn alone and combined with AZT increased MUC1 mRNA expression of Calu-3 and H322M, especially high-dose Zn. Both ACE2 suppression and increased MUC1 mRNA expression were consistently demonstrated in the two human

airway cells, indicating the prophylactic and early therapeutic potential of AZT and Zn repurposing combination for COVID-19. However, further preclinical studies and clinical trials must be performed for validation before clinical decision making.

In vitro cell line exploration using two representative human airway cells is the limitation of this study. If we can verify in animal experiments and compare with actual patient samples, the results will increase clinical application value.

5. Conclusions

This study demonstrated in vitro proof of concept for IκBα associated rapid and synergistic suppression of the key viral entry molecule, ACE2, following combination treatments of clinically repurposed AZT plus zinc early in COVID-19 outbreak. Taking regulatory potential of AZT plus Zn on MUC1 of human airway cells, such clinical repurposing could be considered early in COVID-19 disease course.

Author Contributions: Conceptualization, Y.-K.C. and M.-C.L.; methodology, Y.-K.C. and M.-C.L.; formal analysis, Y.-K.C., C.-W.C., C.-Y.C. and T.-T.H.; investigation, Y.-K.C., C.-W.C., Y.-P.L., Y.-J.H. and T.-T.H.; data curation, C.-Y.C. and B.-R.L.; writing—original draft preparation, Y.-K.C., C.-W.C. and T.-T.H.; writing—review and editing, Y.-K.C., C.-W.C. and T.-T.H.; supervision, Y.-K.C. and T.-T.H.; project administration, Y.-K.C. and T.-T.H. All authors have read and agreed to the published version of the manuscript.

Funding: This research received no external funding.

Institutional Review Board Statement: Ethical review and approval were waived for this study, due to in vitro cell line study only without biohazard material.

Informed Consent Statement: Not applicable.

Data Availability Statement: Any further information will be available from the corresponding authors on request.

Acknowledgments: We are grateful to Ann-Lii Cheng (Dean of National Taiwan University Cancer Center) and Ming-Hua Shiao, Yao-Joe Joseph Yang (Chiefs of Taiwan Instrument Research Institute, National Applied Research Laboratories) for organization and coordination between the groups. We thank staff of the Second Core Lab, Department of Medical Research, National Taiwan University Hospital for technical support during the study. We thank Chao-Chi Ho (National Taiwan University Hospital) for technical support of lung cancer cell lines.

Conflicts of Interest: The authors declare no conflict of interest. All cell lines and experiments were in accordance with the Declaration of Helsinki.

References

1. Zhou, P.; Yang, X.L.; Wang, X.G.; Hu, B.; Zhang, L.; Zhang, W.; Si, H.R.; Zhu, Y.; Li, B.; Huang, C.L.; et al. A pneumonia outbreak associated with a new coronavirus of probable bat origin. *Nature* **2020**, *579*, 270–273. [[CrossRef](#)]
2. Hoffmann, M.; Kleine-Weber, H.; Schroeder, S.; Kruger, N.; Herrler, T.; Erichsen, S.; Schiergens, T.S.; Herrler, G.; Wu, N.H.; Nitsche, A.; et al. SARS-CoV-2 Cell Entry Depends on ACE2 and TMPRSS2 and Is Blocked by a Clinically Proven Protease Inhibitor. *Cell* **2020**, *181*, 271–280.e278. [[CrossRef](#)]
3. Walls, A.C.; Park, Y.J.; Tortorici, M.A.; Wall, A.; McGuire, A.T.; Veesler, D. Structure, Function, and Antigenicity of the SARS-CoV-2 Spike Glycoprotein. *Cell* **2020**, *181*, 281–292.e286. [[CrossRef](#)]
4. Zhang, H.; Rostami, M.R.; Leopold, P.L.; Mezey, J.G.; O’Beirne, S.L.; Strulovici-Barel, Y.; Crystal, R.G. Expression of the SARS-CoV-2 ACE2 Receptor in the Human Airway Epithelium. *Am. J. Respir. Crit. Care Med.* **2020**, *202*, 219–229. [[CrossRef](#)]
5. Smith, J.C.; Sausville, E.L.; Girish, V.; Yuan, M.L.; Vasudevan, A.; John, K.M.; Sheltzer, J.M. Cigarette Smoke Exposure and Inflammatory Signaling Increase the Expression of the SARS-CoV-2 Receptor ACE2 in the Respiratory Tract. *Dev. Cell* **2020**, *53*, 514–529.e513. [[CrossRef](#)]
6. Hou, Y.J.; Okuda, K.; Edwards, C.E.; Martinez, D.R.; Asakura, T.; Dinnon, K.H., 3rd; Kato, T.; Lee, R.E.; Yount, B.L.; Mascenik, T.M.; et al. SARS-CoV-2 Reverse Genetics Reveals a Variable Infection Gradient in the Respiratory Tract. *Cell* **2020**, *182*, 429–446.e414. [[CrossRef](#)]
7. Hirano, T.; Murakami, M. COVID-19: A New Virus, but a Familiar Receptor and Cytokine Release Syndrome. *Immunity* **2020**, *52*, 731–733. [[CrossRef](#)]

8. Huang, J.; Hume, A.J.; Abo, K.M.; Werder, R.B.; Villacorta-Martin, C.; Alysandratos, K.D.; Beermann, M.L.; Simone-Roach, C.; Lindstrom-Vautrin, J.; Olejnik, J.; et al. SARS-CoV-2 Infection of Pluripotent Stem Cell-Derived Human Lung Alveolar Type 2 Cells Elicits a Rapid Epithelial-Intrinsic Inflammatory Response. *Cell Stem. Cell* **2020**. [[CrossRef](#)] [[PubMed](#)]
9. Contoli, M.; Papi, A.; Tomassetti, L.; Rizzo, P.; Vieceli Dalla Sega, F.; Fortini, F.; Torsani, F.; Morandi, L.; Ronzoni, L.; Zucchetti, O.; et al. Blood Interferon-alpha Levels and Severity, Outcomes, and Inflammatory Profiles in Hospitalized COVID-19 Patients. *Front. Immunol.* **2021**, *12*, 648004. [[CrossRef](#)]
10. Pfeffer, L.M. The role of nuclear factor kappaB in the interferon response. *J. Interferon. Cytokine Res.* **2011**, *31*, 553–559. [[CrossRef](#)]
11. Mitchell, S.; Mercado, E.L.; Adelaja, A.; Ho, J.Q.; Cheng, Q.J.; Ghosh, G.; Hoffmann, A. An NFkappaB Activity Calculator to Delineate Signaling Crosstalk: Type I and II Interferons Enhance NFkappaB via Distinct Mechanisms. *Front. Immunol.* **2019**, *10*, 1425. [[CrossRef](#)]
12. Mantlo, E.; Bukreyeva, N.; Maruyama, J.; Paessler, S.; Huang, C. Antiviral activities of type I interferons to SARS-CoV-2 infection. *Antiviral. Res.* **2020**, *179*, 104811. [[CrossRef](#)]
13. Ziegler, C.G.K.; Allon, S.J.; Nyquist, S.K.; Mbanjo, I.M.; Miao, V.N.; Tzouanas, C.N.; Cao, Y.; Yousif, A.S.; Bals, J.; Hauser, B.M.; et al. SARS-CoV-2 Receptor ACE2 Is an Interferon-Stimulated Gene in Human Airway Epithelial Cells and Is Detected in Specific Cell Subsets across Tissues. *Cell* **2020**, *181*, 1016–1035.e1019. [[CrossRef](#)] [[PubMed](#)]
14. Harvey, W.T.; Carabelli, A.M.; Jackson, B.; Gupta, R.K.; Thomson, E.C.; Harrison, E.M.; Ludden, C.; Reeve, R.; Rambaut, A.; Consortium, C.-G.U.; et al. SARS-CoV-2 variants, spike mutations and immune escape. *Nat. Rev. Microbiol.* **2021**, *19*, 409–424. [[CrossRef](#)]
15. Zhou, L.; Huntington, K.; Zhang, S.; Carlsen, L.; So, E.Y.; Parker, C.; Sahin, I.; Safran, H.; Kamle, S.; Lee, C.M.; et al. MEK inhibitors reduce cellular expression of ACE2, pERK, pRb while stimulating NK-mediated cytotoxicity and attenuating inflammatory cytokines relevant to SARS-CoV-2 infection. *Oncotarget* **2020**, *11*, 4201–4223. [[CrossRef](#)]
16. Takahashi, Y.; Hayakawa, A.; Sano, R.; Fukuda, H.; Harada, M.; Kubo, R.; Okawa, T.; Kominato, Y. Histone deacetylase inhibitors suppress ACE2 and ABO simultaneously, suggesting a preventive potential against COVID-19. *Sci. Rep.* **2021**, *11*, 3379. [[CrossRef](#)] [[PubMed](#)]
17. Cavalcanti, A.B.; Zampieri, F.G.; Rosa, R.G.; Azevedo, L.C.P.; Veiga, V.C.; Avezum, A.; Damiani, L.P.; Marcadenti, A.; Kawano-Dourado, L.; Lisboa, T.; et al. Hydroxychloroquine with or without Azithromycin in Mild-to-Moderate COVID-19. *N. Engl. J. Med.* **2020**. [[CrossRef](#)]
18. Gautret, P.; Lagier, J.C.; Parola, P.; Hoang, V.T.; Meddeb, L.; Sevestre, J.; Mailhe, M.; Doudier, B.; Aubry, C.; Amrane, S.; et al. Clinical and microbiological effect of a combination of hydroxychloroquine and azithromycin in 80 COVID-19 patients with at least a six-day follow up: A pilot observational study. *Travel Med. Infect. Dis.* **2020**, *34*, 101663. [[CrossRef](#)]
19. Lagier, J.C.; Million, M.; Gautret, P.; Colson, P.; Cortaredona, S.; Giraud-Gatineau, A.; Honore, S.; Gaubert, J.Y.; Fournier, P.E.; Tissot-Dupont, H.; et al. Outcomes of 3,737 COVID-19 patients treated with hydroxychloroquine/azithromycin and other regimens in Marseille, France: A retrospective analysis. *Travel Med. Infect. Dis.* **2020**, 101791. [[CrossRef](#)]
20. Rosenberg, E.S.; Dufort, E.M.; Udo, T.; Wilberschied, L.A.; Kumar, J.; Tesoriero, J.; Weinberg, P.; Kirkwood, J.; Muse, A.; DeHovitz, J.; et al. Association of Treatment With Hydroxychloroquine or Azithromycin With In-Hospital Mortality in Patients With COVID-19 in New York State. *JAMA* **2020**. [[CrossRef](#)]
21. Group, R.C. Azithromycin in patients admitted to hospital with COVID-19 (RECOVERY): A randomised, controlled, open-label, platform trial. *Lancet* **2021**, *397*, 605–612. [[CrossRef](#)]
22. Group, P.T.C. Azithromycin for community treatment of suspected COVID-19 in people at increased risk of an adverse clinical course in the UK (PRINCIPLE): A randomised, controlled, open-label, adaptive platform trial. *Lancet* **2021**, *397*, 1063–1074. [[CrossRef](#)]
23. Million, M.; Lagier, J.C.; Gautret, P.; Colson, P.; Fournier, P.E.; Amrane, S.; Hocquart, M.; Mailhe, M.; Esteves-Vieira, V.; Doudier, B.; et al. Early treatment of COVID-19 patients with hydroxychloroquine and azithromycin: A retrospective analysis of 1061 cases in Marseille, France. *Travel Med. Infect. Dis.* **2020**, *35*, 101738. [[CrossRef](#)]
24. Furtado, R.H.M.; Berwanger, O.; Fonseca, H.A.; Correa, T.D.; Ferraz, L.R.; Lapa, M.G.; Zampieri, F.G.; Veiga, V.C.; Azevedo, L.C.P.; Rosa, R.G.; et al. Azithromycin in addition to standard of care versus standard of care alone in the treatment of patients admitted to the hospital with severe COVID-19 in Brazil (COALITION II): A randomised clinical trial. *Lancet* **2020**, *396*, 959–967. [[CrossRef](#)]
25. Finzi, E. Treatment of SARS-CoV-2 with high dose oral zinc salts: A report on four patients. *Int. J. Infect. Dis.* **2020**, *99*, 307–309. [[CrossRef](#)]
26. Carlucci, P.M.; Ahuja, T.; Petrilli, C.; Rajagopalan, H.; Jones, S.; Rahimian, J. Zinc sulfate in combination with a zinc ionophore may improve outcomes in hospitalized COVID-19 patients. *J. Med. Microbiol.* **2020**, *69*, 1228–1234. [[CrossRef](#)]
27. Derwand, R.; Scholz, M.; Zelenko, V. COVID-19 outpatients: Early risk-stratified treatment with zinc plus low-dose hydroxychloroquine and azithromycin: A retrospective case series study. *Int. J. Antimicrob. Agents* **2020**, *56*, 106214. [[CrossRef](#)]
28. Self, W.H.; Semler, M.W.; Leither, L.M.; Casey, J.D.; Angus, D.C.; Brower, R.G.; Chang, S.Y.; Collins, S.P.; Eppensteiner, J.C.; Filbin, M.R.; et al. Effect of Hydroxychloroquine on Clinical Status at 14 Days in Hospitalized Patients With COVID-19: A Randomized Clinical Trial. *JAMA* **2020**, *324*, 2165–2176. [[CrossRef](#)] [[PubMed](#)]
29. Group, R.C.; Horby, P.; Mafham, M.; Linsell, L.; Bell, J.L.; Staplin, N.; Emberson, J.R.; Wiselka, M.; Ustianowski, A.; Elmahi, E.; et al. Effect of Hydroxychloroquine in Hospitalized Patients with COVID-19. *N. Engl. J. Med.* **2020**, *383*, 2030–2040. [[CrossRef](#)]

30. Oldenburg, C.E.; Pinsky, B.A.; Brogdon, J.; Chen, C.; Ruder, K.; Zhong, L.; Nyatigo, F.; Cook, C.A.; Hinterwirth, A.; Lebas, E.; et al. Effect of Oral Azithromycin vs Placebo on COVID-19 Symptoms in Outpatients With SARS-CoV-2 Infection: A Randomized Clinical Trial. *JAMA* **2021**, *326*, 490–498. [[CrossRef](#)]
31. Tenson, T.; Lovmar, M.; Ehrenberg, M. The mechanism of action of macrolides, lincosamides and streptogramin B reveals the nascent peptide exit path in the ribosome. *J. Mol. Biol.* **2003**, *330*, 1005–1014. [[CrossRef](#)]
32. Tran, D.H.; Sugamata, R.; Hirose, T.; Suzuki, S.; Noguchi, Y.; Sugawara, A.; Ito, F.; Yamamoto, T.; Kawachi, S.; Akagawa, K.S.; et al. Azithromycin, a 15-membered macrolide antibiotic, inhibits influenza A(H1N1)pdm09 virus infection by interfering with virus internalization process. *J. Antibiot.* **2019**, *72*, 759–768. [[CrossRef](#)]
33. Gielen, V.; Johnston, S.L.; Edwards, M.R. Azithromycin induces anti-viral responses in bronchial epithelial cells. *Eur. Respir. J.* **2010**, *36*, 646–654. [[CrossRef](#)] [[PubMed](#)]
34. Schogler, A.; Kopf, B.S.; Edwards, M.R.; Johnston, S.L.; Casaulta, C.; Kieninger, E.; Jung, A.; Moeller, A.; Geiser, T.; Regamey, N.; et al. Novel antiviral properties of azithromycin in cystic fibrosis airway epithelial cells. *Eur. Respir. J.* **2015**, *45*, 428–439. [[CrossRef](#)] [[PubMed](#)]
35. Menzel, M.; Akbarshahi, H.; Bjermer, L.; Uller, L. Azithromycin induces anti-viral effects in cultured bronchial epithelial cells from COPD patients. *Sci. Rep.* **2016**, *6*, 28698. [[CrossRef](#)]
36. Stellari, F.F.; Sala, A.; Donofrio, G.; Ruscitti, F.; Caruso, P.; Topini, T.M.; Francis, K.P.; Li, X.; Carnini, C.; Civelli, M.; et al. Azithromycin inhibits nuclear factor-kappaB activation during lung inflammation: An in vivo imaging study. *Pharmacol. Res. Perspect.* **2014**, *2*, e00058. [[CrossRef](#)] [[PubMed](#)]
37. Aghai, Z.H.; Kode, A.; Saslow, J.G.; Nakhla, T.; Farhath, S.; Stahl, G.E.; Eydelman, R.; Strande, L.; Leone, P.; Rahman, I. Azithromycin suppresses activation of nuclear factor-kappa B and synthesis of pro-inflammatory cytokines in tracheal aspirate cells from premature infants. *Pediatr. Res.* **2007**, *62*, 483–488. [[CrossRef](#)] [[PubMed](#)]
38. Wessels, I.; Rolles, B.; Rink, L. The Potential Impact of Zinc Supplementation on COVID-19 Pathogenesis. *Front. Immunol.* **2020**, *11*, 1712. [[CrossRef](#)] [[PubMed](#)]
39. Gau, J.T.; Ebersbacher, C.; Kao, T.C. Serum Zinc Concentrations of Adults in an Outpatient Clinic and Risk Factors Associated With Zinc Deficiency. *J. Am. Osteopath. Assoc.* **2020**, *120*, 796–805. [[CrossRef](#)] [[PubMed](#)]
40. Jothimani, D.; Kailasam, E.; Danielraj, S.; Nallathambi, B.; Ramachandran, H.; Sekar, P.; Manoharan, S.; Ramani, V.; Narasimhan, G.; Kaliamoorthy, I.; et al. COVID-19: Poor outcomes in patients with zinc deficiency. *Int. J. Infect. Dis.* **2020**, *100*, 343–349. [[CrossRef](#)]
41. Kumar, A.; Kubota, Y.; Chernov, M.; Kasuya, H. Potential role of zinc supplementation in prophylaxis and treatment of COVID-19. *Med. Hypotheses* **2020**, *144*, 109848. [[CrossRef](#)]
42. Sahebnaasagh, A.; Saghafi, F.; Avan, R.; Khoshi, A.; Khataminia, M.; Safdari, M.; Habtemariam, S.; Ghaleno, H.R.; Nabavi, S.M. The prophylaxis and treatment potential of supplements for COVID-19. *Eur. J. Pharmacol.* **2020**, *887*, 173530. [[CrossRef](#)]
43. Bao, S.; Liu, M.J.; Lee, B.; Besecker, B.; Lai, J.P.; Guttridge, D.C.; Knoell, D.L. Zinc modulates the innate immune response in vivo to polymicrobial sepsis through regulation of NF-kappaB. *Am. J. Physiol. Lung Cell Mol. Physiol.* **2010**, *298*, L744–L754. [[CrossRef](#)]
44. Pelaseyed, T.; Bergstrom, J.H.; Gustafsson, J.K.; Ermund, A.; Birchenough, G.M.; Schutte, A.; van der Post, S.; Svensson, F.; Rodriguez-Pineiro, A.M.; Nystrom, E.E.; et al. The mucus and mucins of the goblet cells and enterocytes provide the first defense line of the gastrointestinal tract and interact with the immune system. *Immunol. Rev.* **2014**, *260*, 8–20. [[CrossRef](#)]
45. Lu, W.; Liu, X.; Wang, T.; Liu, F.; Zhu, A.; Lin, Y.; Luo, J.; Ye, F.; He, J.; Zhao, J.; et al. Elevated MUC1 and MUC5AC mucin protein levels in airway mucus of critical ill COVID-19 patients. *J. Med. Virol.* **2021**, *93*, 582–584. [[CrossRef](#)] [[PubMed](#)]
46. Liu, Y.; Lv, J.; Liu, J.; Li, M.; Xie, J.; Lv, Q.; Deng, W.; Zhou, N.; Zhou, Y.; Song, J.; et al. Mucus production stimulated by IFN-AhR signaling triggers hypoxia of COVID-19. *Cell Res* **2020**, *30*, 1078–1087. [[CrossRef](#)] [[PubMed](#)]
47. Sbinovska, N.; Zakelj, S.; Roskar, R.; Kristan, K. Suitability and functional characterization of two Calu-3 cell models for prediction of drug permeability across the airway epithelial barrier. *Int. J. Pharm.* **2020**, *585*, 119484. [[CrossRef](#)] [[PubMed](#)]
48. Foster, K.A.; Avery, M.L.; Yazdanian, M.; Audus, K.L. Characterization of the Calu-3 cell line as a tool to screen pulmonary drug delivery. *Int. J. Pharm.* **2000**, *208*, 1–11. [[CrossRef](#)]
49. Inoue, D.; Furubayashi, T.; Tanaka, A.; Sakane, T.; Sugano, K. Quantitative estimation of drug permeation through nasal mucosa using in vitro membrane permeability across Calu-3 cell layers for predicting in vivo bioavailability after intranasal administration to rats. *Eur. J. Pharm. Biopharm.* **2020**, *149*, 145–153. [[CrossRef](#)]
50. Liao, M.; Liu, Y.; Yuan, J.; Wen, Y.; Xu, G.; Zhao, J.; Cheng, L.; Li, J.; Wang, X.; Wang, F.; et al. Single-cell landscape of bronchoalveolar immune cells in patients with COVID-19. *Nat. Med.* **2020**, *26*, 842–844. [[CrossRef](#)]
51. Xu, G.; Qi, F.; Li, H.; Yang, Q.; Wang, H.; Wang, X.; Liu, X.; Zhao, J.; Liao, X.; Liu, Y.; et al. The differential immune responses to COVID-19 in peripheral and lung revealed by single-cell RNA sequencing. *Cell Discov.* **2020**, *6*, 73. [[CrossRef](#)] [[PubMed](#)]
52. Perera, M.; El Khoury, J.; Chinni, V.; Bolton, D.; Qu, L.; Johnson, P.; Trubiano, J.; McDonald, C.F.; Jones, D.; Bellomo, R.; et al. Randomised controlled trial for high-dose intravenous zinc as adjunctive therapy in SARS-CoV-2 (COVID-19) positive critically ill patients: Trial protocol. *BMJ Open* **2020**, *10*, e040580. [[CrossRef](#)]

-
53. Patel, O.; Chinni, V.; El-Khoury, J.; Perera, M.; Neto, A.S.; McDonald, C.; See, E.; Jones, D.; Bolton, D.; Bellomo, R.; et al. A pilot double-blind safety and feasibility randomized controlled trial of high-dose intravenous zinc in hospitalized COVID-19 patients. *J. Med. Virol.* **2021**, *93*, 3261–3267. [[CrossRef](#)]
 54. Mathes, E.; O’Dea, E.L.; Hoffmann, A.; Ghosh, G. NF-kappaB dictates the degradation pathway of IkappaBalpha. *EMBO J.* **2008**, *27*, 1357–1367. [[CrossRef](#)] [[PubMed](#)]